DESIGN AND EXPERIMENTATION OF A PERSONAL PENDULUM VEHICLE

M. Fiacchini * **A. Viguria** * **R. Cano** * **A. Prieto** *
F.R. Rubio * **J. Aracil** * **C. Canudas-de-Wit** **

* *Dept. Ingeniería de Sistemas y Automática, Universidad de Sevilla, Spain*
** *Lab. d'Automatique, Grenoble (CNRS-LAG), France*

Abstract: This paper describes the development of a vehicle based on the stabilization of an inverted pendulum. The prototype has been designed and developed by the School of Engineering of Seville using commercial and low-cost components. Two vehicle controllers (linear and nonlinear) have been developed and applied. Moreover, they have been tested successfully in various experiments. ***

*** This project won the Schneider Electric (Spain) "Innovation and Development of Automation Systems" award.

Keywords: Inverted pendulum, nonlinear control, real time.

1. INTRODUCTION

Inverted pendulum control is a classic problem within the field of nonlinear control. There are several variations of the problem, the main ones are: the Furuta pendulum (Furuta, 2003), (Aström and Furuta, 1996), the pendulum on a mobile cart (Gordillo *et al.*, 2004) and, more recently, the pendulum on a two-wheeled vehicle with independent motors (Baloh and Parent, 2003), (Grasser *et al.*, 2002), (Segway, 2004). In addition, there is a wide range of controller systems, designed throughout the last few decades for these applications. Because of the practical nature of this project and the limited cost of the components used, only those controllers which require not many calculations have been selected.

This paper focuses on the problem of an inverted pendulum on a two-wheeled vehicle for human transportation (Figure 1), where the pendulum is actually the person riding the vehicle. The forward movement is caused by the rider's inclination with respect to the equilibrium position. In fact, the controllers shown in Section 4 were designed taking into account only their straight-line movement, while the rotation movement is controlled through a command set by the driver through an electric device.

Fig. 1. General view of the vehicle

The core of the system is made up of a microcontroller, whose function is to calculate the controller's actions using the information arriv-

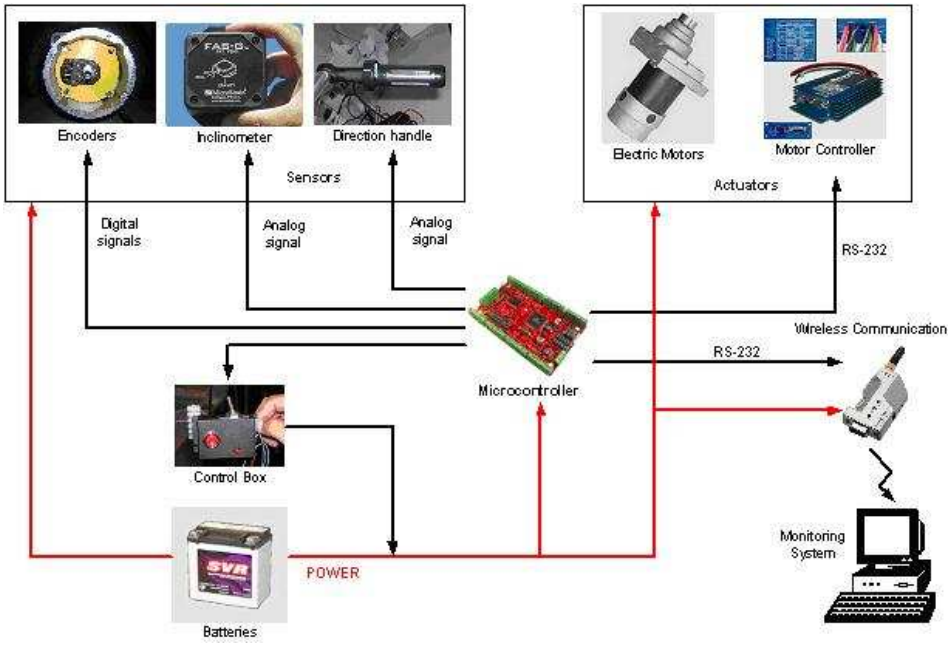

Fig. 2. Architecture of the system

ing from the various sensors. This microcontroller communicates with a PC, allowing the online controller adjustment, and it also collects relevant vehicle data for future research. These features allow the study of various control techniques, through the performance of simple experiments.

This paper is organized as follows. Section 2 describes the different components that make up the system, and the relationship between them, both at a hardware and a software level. Section 3 shows the platform model used in Section 4 for the controller design phase. Section 5 presents the results obtained both in the simulation and in the experiments that were carried out. The last section is made up of conclusions and possible future developments.

2. ARCHITECTURE OF THE SYSTEM

The system has an 8-bit, low-cost microcontroller (Atmega128, by Atmel), which communicates with the various peripherals. As it can be seen in Figure 2, there are two sets of devices connected to the microcontroller: sensors and actuators. The set of sensors is made up, first of all, by an encoder for each wheel, which have been used on the vehicle to measure their rotation speed. The second element of the sensor set is a MicroStrain inclinometer, which does preprocessing of the signal based on a Kalman filter. Although the processed signal shows good qualities, it is necessary to put a filter underneath in order to reduce the noise, as shown in Section 5. The last sensor indicates the reference direction the rider wants to go. This reference is indicated through a grip with an electric interface. The system actuators are two electric motors that run on 24V and are able to reach 240 rpm. The electric power that these motors need is supplied by a RoboteQ motor controller, which communicates with the microcontroller through a standard RS-232 and a communications protocol.

For the auxiliary equipment, one of the main features is the Bluetooth wireless link. This link allows to have a wireless connection between the microcontroller and the monitoring PC. The control box makes possible to do the following: to turn the system on and off, to easily know the microcontroller's state through a led and it includes a security mechanism, featuring a switch that must be pressed as long as the controller is active. As soon as the switch is not pressed, the controller will stop working, bringing the vehicle to a halt.

The software for the microcontroller was based on the TinyOS operating system for embedded systems (Hill *et al.*, 2000), developed at UC Berkeley. To carry out useful experiments, it is necessary to have a reliable way to monitor and store the data they generate. This is the reason behind the development of a PC software application, with the aim of: monitoring the system variables in real time, storing the samples obtained in the experiment for subsequent study, changing the controller state (stop, active, emergency stop) and having the possibility of changing the controller's parameters in a simple way, without having to reprogram the microcontroller.

The communications protocol is made up of a series of interface frames, where the PC controls the communications and the microcontroller only re-

sponds to its requests. Several XML-based graphic templates have been created in order to facilitate the downloading of the various controllers and provide a simple way to change their parameters.

3. SYSTEM MODEL

The system is basically made up of a platform that is mounted on two wheels activated independently by two engines. On this platform, there is a mass that can be represented as a mass point at a distance l from the base plane. Figure 3 shows a diagram of the vehicle structure, the reference axis, degrees of freedom and system connections. From the control point of view, the system may be

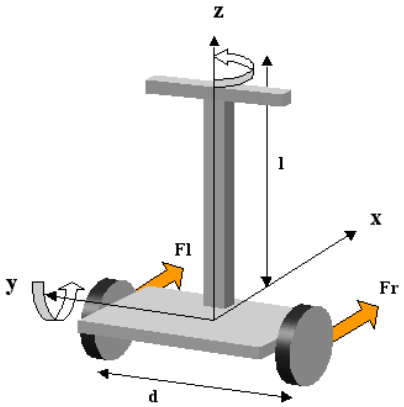

Fig. 3. Vehicle configuration diagram

divided into two subsystems, which are practically decoupled. One of them is formed by a mobile robot with differential traction, while the other is made up of an inverted pendulum on a mobile cart.

3.1 Differential traction vehicle

The variable output of this system is the revolution speed with respect to the vertical axis. Its reference is given by a signal that comes from the vehicle's direction grip.

Considering the forces exerted by each wheel, F_l and F_r, the vehicle equations can by obtained as follows,

$$J\,\ddot{\delta} = (F_r - F_l)\,d, \tag{1}$$

where:

- F_l and F_r $[N]$: force exerted by the left and right wheels respectively,
- $J = 10\ kg\,m^2$: inertial momentum with respect to the vertical axis,
- $\ddot{\delta}$ $[rad/s^2]$: angular acceleration around axis z,
- $d = 0.83\ m$: distance between the wheels.

3.2 Inverted pendulum on a mobile base

Figure 4 represents the subsystem made up of the inverted pendulum on a mobile platform. The

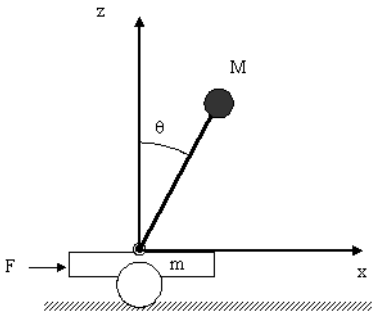

Fig. 4. Inverted pendulum on a mobile car

equilibrium of forces on the axis x can be seen in the following equation:

$$(M+m)\ddot{x} + Ml\ddot{\theta}\cos\theta = F, \tag{2}$$

where $F = F_l + F_r$.

On the other hand, the equilibrium of momenta around the pendulum's turning point leads to

$$\ddot{x}Ml\cos\theta + Ml^2\ddot{\theta} - Mgl\sin\theta = 0, \tag{3}$$

where:

- $m = 35\ kg$: mass of the cart,
- $M = 70\ kg$: mass of the pendulum,
- $l = 1\ m$: height of the center of mass,
- $g = 9.8\ m/s^2$: gravity acceleration.

Since the aim of the controller is to stabilize the angle at zero and the linear velocity $\dot{x} = v$, the interesting variables of the system are: the angle θ, the angular velocity $\dot{\theta}$ and the linear velocity v.

4. CONTROLLER DESIGN

This section describes both controller methods used for this system. The first one is a LQR (Linear Quadratic Regulator), a linear controller that requires a linear system model around a equilibrium point. The other is a nonlinear controller, whose design is based on the previously obtained differential nonlinear equations.

4.1 LQR controller

The LRQ is a controller for state-variable feedback in such a way that

$$u = -Kx, \tag{4}$$

so that the value of K is obtained from a minimizing problem of the functional cost,

$$J = \int_0^\infty (x'Qx + u'Ru)\mathrm{d}t. \tag{5}$$

Matrixes Q and R penalize the state error and the control effort, respectively.

The system can be linearized around the equilibrium point $\theta = 0$, $\dot{\theta} = 0$ and $v = 0$. At this point, approximations $\cos\theta \approx 1$ and $\sin\theta \approx \theta$ can be performed. Therefore, the resulting state equations are:

$$\begin{pmatrix} \dot{\theta} \\ \ddot{\theta} \\ \dot{v} \end{pmatrix} = \begin{pmatrix} 0 & 1 & 0 \\ \frac{(M+m)g}{ml} & 0 & 0 \\ -\frac{Mg}{m} & 0 & 0 \end{pmatrix} \begin{pmatrix} \theta \\ \dot{\theta} \\ v \end{pmatrix} + \begin{pmatrix} 0 \\ -\frac{1}{ml} \\ \frac{1}{m} \end{pmatrix} F. \tag{6}$$

Using this model, the solution of the LQR problem produces the following controller:

$$F = -K_1\theta - K_2\dot{\theta} - K_3 v, \tag{7}$$

where parameters K_1, K_2 and K_3 are determined according to the values of matrix elements Q and R of expression (5).

4.2 Nonlinear Controller

The nonlinear controller design was developed in several phases. First of all, a partial linearization of the system equations was obtained. Then, the subsystem pendulum was stabilized through the energy shaping function, to finally stabilize the linear velocity of the vehicle through the controller proposed by Astolfil-Kaliora (Kaliora and Astolfi, 2004). Each of these phases has been described in the following subsections.

4.2.1. Partial Linearization Defining a new control variable

$$u = \frac{F + Ml\dot{\theta}^2 \sin\theta - Mg\sin\theta\cos\theta}{(M+m) - M\cos^2\theta}, \tag{8}$$

equations (2) and (3) of the model can be rewritten as follows:

$$\begin{array}{l} u\cos\theta + l\ddot{\theta} - g\sin\theta = 0 \\ \ddot{x} = u \end{array}, \tag{9}$$

So the system state equations result in

$$\begin{array}{rcl} \dot{x_1} & = & x_2 \\ \dot{x_2} & = & \dfrac{g\sin x_1 - u\cos x_1}{l}, \\ \dot{x_3} & = & u \end{array} \tag{10}$$

where $x_1 = \theta$, $x_2 = \dot{\theta}$, $x_3 = \dot{x}$.

The system now has a cascading structure that allows to obtain a scaled solution to the control problem.

4.2.2. Energy shaping function There are several ways to stabilize the pendulum. One of them is to modify the energy shape of the system, using a control law, so that only its minimum coincides with the point to be stabilized.

To obtain this control law, it is sufficient to make equal the inverted pendulum equations and the non-inverted ones, resulting in

$$u = 2g\tan x_1. \tag{11}$$

Using this control law, the system would show oscillations around the equilibrium point. If an asymptotically stationary behavior is desired, it is necessary to add a damping element whose friction constant is K_a.

$$u = 2K_m g\tan x_1 + \frac{K_a}{M}x_2, \tag{12}$$

where K_m is a constant that adds a wider degree of freedom adjustment for the controller.

4.2.3. Velocity stabilization Once the pendulum has been stabilized and since the system has a cascading structure using partial linearization, *forwarding* techniques can be applied to stabilize the vehicle speed. Thus, the goal can be reached by adding a new element to the control law, so that

$$u = 2K_m g\tan x_1 + \frac{K_a}{M}x_2 + u_d\ . \tag{13}$$

The value of u_d can be obtained as in (Gordillo *et al.*, 2004). However in this paper, because of the simplicity of its calculations, the control that has been used is the one proposed by Astolfi-Kaliora (Kaliora and Astolfi, 2004), where

$$u_d = \epsilon\,\mathrm{sat}\left(\frac{K_v x_3}{\epsilon}\right). \tag{14}$$

and the parameters K_v and ϵ are empirically set.

Thus, undoing the partial linearization, the global control law indicates that the force to apply to the cart, in order to obtain pendulum and vehicle speed stabilization, results in

$$\begin{array}{c} F = \left[(M+m) - M\cos^2\theta\right]u + \\ Mg\sin\theta\cos\theta - Ml\dot{\theta}^2\sin\theta \end{array}, \tag{15}$$

with

$$u = 2K_m g \tan\theta + \frac{K_a}{M}\dot{\theta} + \epsilon \,\mathrm{sat}\left(\frac{K_v v}{\epsilon}\right). \quad (16)$$

4.2.4. Nonlinear Controller Tuning The LQR controller has an optimal behavior around the equilibrium point. Therefore, if the relation between this controller's constants and the Astolfi-Kaliora controller's constants is established, values K_m, K_a and K_v can be obtained to provide a behavior similar to LQR, at least near the equilibrium point is concerned.

When the nonlinear control expressions, (15) and (16), are linearized at the equilibrium point ($\theta = 0$, $\dot{\theta} = 0$ and $v = 0$) the following equation is obtained,

$$F = [Mg + 2gmK_m]\theta + mK_a\dot{\theta} + mK_v v. \quad (17)$$

Comparing this equation with the LQR equation, (7), values K_m, K_a and K_v can be obtained, which will provide a controller with appreciate features, thus

$$K_m = \frac{-K_1 - Mg}{2gm}$$
$$K_a = \frac{-K_2}{m}; \qquad K_v = \frac{-K_3}{m} \quad (18)$$

5. SIMULATION AND EXPERIMENTAL RESULTS

Having completed the controller design, a set of simulations was made with the Matlab-Simulink tool. This allows to check its operation and to fine-tune the various parameters of commented controllers. The signal that comes from the controller, corresponding to the force to apply to the cart, is spread in a symmetric way between the two wheels of the vehicle. Moreover, vehicle

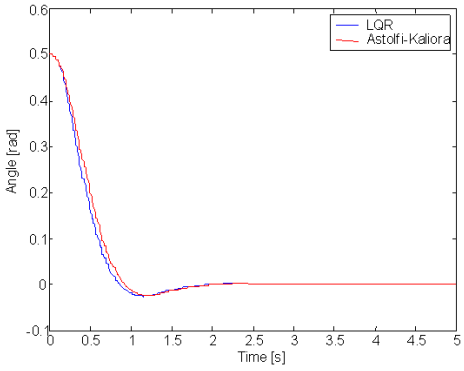

Fig. 5. Controller comparison

steering is obtained using a proportional control that increases the force exerted on one of the wheels while decreasing it on the other, producing the desired turning.

The Riccati equation associated with the LQR problem has been solved to calculate the linear controller's parameters using the following matrixes

$$Q = \begin{bmatrix} 100 & 0 & 0 \\ 0 & 100 & 0 \\ 0 & 0 & 1 \end{bmatrix} \qquad R = 0.1\,, \quad (19)$$

in equation (5), which produces the following values,

$$K_1 = 2070 \qquad K_2 = 385.1 \qquad K_3 = 3.2 \quad (20)$$

Using the fine-tuning equations (18) the nonlinear controller's parameters are,

$$K_m = -4.017 \quad K_a = -11.004 \quad K_v = -0.090 \quad (21)$$

The simulations made with these parameters show that both controllers, LQR and nonlinear, present a very similar behavior around the equilibrium point. Only when the pendulum moves away from the vertical position differences can be noticed. Figure 5 shows the angle evolution, with both controllers, starting at an initial position of 0.5 rad, until the stabilization at zero.

When these controllers were used in the vehicles, a strong vibration was noticed because of noise in the inclinometer signal. The effect of this noise can be seen on the feedback of the measurement of angle θ and especially of its derivative $\dot{\theta}$, since it is calculated according to the increase of the signal in the sample time. Since the sampling time is very short, 10 ms, the rapid variations caused by the noise produce very high values in the derivative. To lessen this feature, two elements

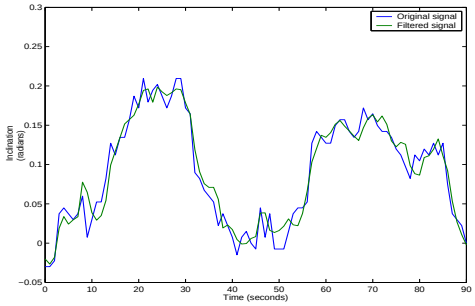

Fig. 6. Comparison of original and filtered θ signal

can be adjusted: applying a filter to the signal to eliminate the high frequency components caused by the noise and reducing the value of the constant of feedback state $\dot{\theta}$. Both effects are shown in Figs. 6 and 7.

Specifically, a second order Butterworth filter was applied, using IIR (Infinite Impulse Response) filter design technology, through bilinear transformation (Ifeachor and Barrie, 1993). The transfer function of the bilinear filter used is:

$$H(z^{-1}) = \frac{0.0133z^{-2} + 0.0266z^{-1} + 0.0133}{0.85z^{-2} - 1.9734z^{-1} + 1.1766}. \quad (22)$$

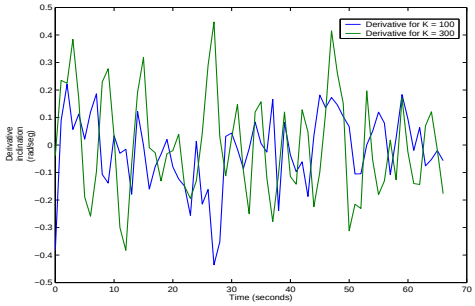

Fig. 7. Noise intensification in $\dot{\theta}$ increasing K_2

Finally, a satisfactory behavior was observed, by setting $K_2 = 100$ for the LQR, and calculating the corresponding K_a for the nonlinear controller. Figures 8 and 9 show the forces associated to each of the vehicle wheels for both controllers used. Both figures show the same experiment where, at first the vehicle moves forward, then it turns around once and, finally, it moves forward turning left and right.

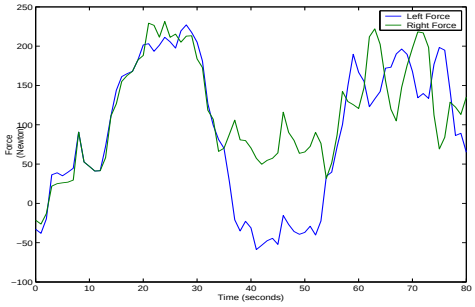

Fig. 8. Experiment results with LQR controller

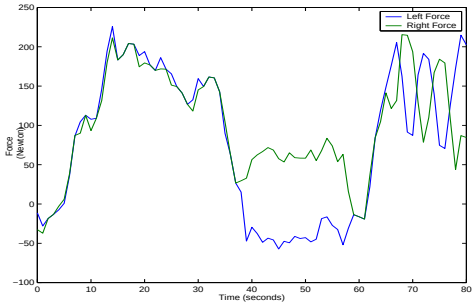

Fig. 9. Experiment results with nonlinear controller

The experimental comparison between both controllers has not provided results that show the differences between them, since it is not possible to repeat exactly the same experiment because of the driver.

6. CONCLUSIONS AND FUTURE WORKS

This paper presents a vehicle whose behavior is based on the stabilization of an inverted pendulum. This vehicle has been manufactured using low-cost commercial components. An experimentation system has been obtained and allows to test various controllers.

Two types of controllers were used in the tests performed: an optimal linear controller (LQR) and a nonlinear controller based on energy shaping, having accomplished a comfortable and smooth drive in both cases.

Future developments will include designing new control techniques and performing a comparative study among them. Finally, several demonstration videos are available on the following webpage: http://nyquist.us.es/∼ppcar.

ACKNOWLEDGEMENTS

The authors would like to acknowledge MCYT for funding this work under grants DPI2004-06419, DPI2003-00429, HF2003-0237 and SAB2003-0085. Thanks are also due to the programm PICASSO No. 07261YJ(EGIDE), of the French Minister of foreign affaires. Thanks are also due to Benito J. Vela for their contribution in the mechanical of the vehicle.

REFERENCES

Aström, K. J. and K. Furuta (1996). Swinging-up a pendulum by energy control. In: *Proc. IFAC Congress*. pp. 37–95.

Baloh, M. and M. Parent (2003). Modeling and model verification intelligent self-balancing two-wheeled vehicle for an autonomous urban transportation system. In: *Conf. Comp. Intelligence, Robotics Autonomous Systems*. Singapore.

Furuta, K. (2003). Control of pendulum: From super mechano-system to human adaptative mechatronics. In: *Proceedings of the 42nd IEEE CDC*.

Gordillo, F., F. Salas and J. Aracil (2004). A forwarding controller for the pendulum on a cart. In: *Proceedings of Controlo*. Vol. 6. Portugal.

Grasser, F., A. D'Arrigo, S. Colombi and A. Rufer (2002). Joe: A mobile, inverted pendulum. *IEEE Trans. Industrial Electronics* **40(1)**, 107–114.

Hill, J., R. Szewczyk, A. Woo, S. Hollar, D. Culler and K. Pister (2000). System architecture directions for networked sensors. *ACM. Operating Systems Review*. **34(5)**, 93–104.

Ifeachor, Emmanuel C. and W. Jervis Barrie (1993). *Digital Signal Processing: A Practical Approach*. Addison-Wesley.

Kaliora, G. and A. Astolfi (2004). Nonlinear control of feedforward systems with bounded signals. *IEEE Trans. Autom. Control* **49(11)**, 1975–1990.

Segway, Inc. (2004). http://www.segway.com.